High pressure theoretical and experimental analysis of the bandgap of $BaMoO_4$, $PbMoO_4$ and $CdMoO_4$

V. Monteseguro,[1,*] J. Ruiz-Fuertes,[2] J. Contreras-García,[3] P. Rodríguez-Hernández,[4] A. Muñoz,[4] and D. Errandonea[1]

[1]*Departamento de Física Aplicada-ICMUV, Universitat de València, Calle Dr. Moliner 50, 46100 Burjassot, Spain*
[2]*DCITIMAC, Universidad de Cantabria, Avenida de los Castros 48, 39005 Santander, Spain*
[3]*CNRS, Laboratoire de Chimie Théorique, LCT, Sorbonne Université, F. 75005 Paris, France*
[4]*Instituto de Materiales y Nanotecnología, Departamento de Física, Universidad de La Laguna, La Laguna, 38205 Tenerife, Spain*

(Dated: June 17, 2019)

We have investigated the origin of the bandgap of the $BaMoO_4$, $PbMoO_4$, and $CdMoO_4$ crystals on the basis of optical absorption spectroscopy experiments and *ab initio* electronic band structure, density of states, and electronic localization function calculations under high pressure. Our study provides an accurate determination of the bandgaps E_g and their pressure derivatives dE_g/dP for $BaMoO_4$ (4.43 eV, -4.4 meV/GPa), $PbMoO_4$ (3.45 eV, -53.8 meV/GPa), and $CdMoO_4$ (3.71 eV, -3.3 meV/GPa). The absorption edges were fitted with the Urbach exponential model which we demonstrate to be the most appropriate on thick crystals with direct bandgaps. So far, the narrowing of the bandgap of distinct $PbMoO_4$ had been qualitatively explained considering only the presence of the Pb $6s$ levels at the top of its valence band. Its fast pressure dependent redshift and the occurrence of its direct bandgap away from Γ in contrast to the other scheelites had remained unsolved. Here we show that contrary to what had been proposed and differently to the other scheelites, in $PbMoO_4$ the band gap takes place between the Pb $6s$ levels at the top of the valence band and the antibonding O $2p$ levels at the bottom of the conduction band. For this reason the direct bandgap is pushed away from zone center in order to allow $s-p$ mixing. Its pressure dependence is one order of magnitude faster than in the other shceelites due to two effects: its delocalized character and the higher compressibility of dodecahedral units, PbO_8, compared to tetrahedral units, MoO_4.

The optical properties of scheelites have interested experimental particle physicists for more than three decades. High light yield emission [1] when hit by high-energy particles or photons, and long decay times due to the creation of self-trapped Frenkel excitons [2], have converted these wide-bandgap scintillating semiconductors into indispensable materials for x-ray detectors in tomography [3] and dosimetry devices [4]. Regarding the optical properties of these compounds, the control and tuning of their bandgaps is a fundamental necessity. It is, though, a complicated issue because doping does not only serve to create secondary levels that influence the electronic density of states near the Fermi level but also create defects and disorder in critical amounts so that the scintillating properties might be eventually worsened. Pressure is an extraordinary tool to probe the effects of changing the bond distances on the electronic structure of semiconductors. The shortening of the bond distances is expected to increase the overlap between neighbouring orbitals, increasing the band dispersion and eventually narrowing the bandgap. The electronic structures and bandgaps of scheelites have been studied in detail in many works [5–7]. In most cases, their direct bandgaps take place at zone center between the O $2p$ and Mo $5d$ levels and are quite pressure-independent showing a small redshift. However, the scenario changes when Pb^{2+} is the divalent metallic cation. In this case, the direct bandgap is severely reduced occurring away from zone center and the bandgap becomes much more pressure sentitive, e. g. -71 meV/GPa for $PbWO_4$ [8] and -50 meV/GPa for $PbMoO_4$ [9]. This is one order of magnitude faster than for the remaining studied scheelites, i.e. the bandgap of $CaWO_4$ varies at -2.1 meV/GPa [7]. Such a different response to pressure between lead-bearing and non-lead-bearing scheelites has been tentatively attributed to the influence of the Pb $6s$ states located at the top of the valence band overlapping with the O $2p$ states [5, 8]. Although the presence of the Pb $6s$ levels at the top of the valence band must have an effect on the strong redshift of the bandgap in $PbWO_4$ and $PbMoO_4$, what particular effect it is has never been explained.

Furthermore, differently to scheelite-type tungstates, an accurate determination in the case of scheelite-type molybdates at ambient pressure is still missing. It is known [7, 10] that the absorption edge of scheelites must be explained according to Urbach's law [10] and an inappropriate $(\alpha h\nu)^2$ analysis can lead to different values depending on the maximum absorption coefficient α measured in the experiment. In fact, a rapid search in the literature provides an enormous dispersion of the bandgap values of scheelite-type molybdates. For example, in $PbMoO_4$ we find experimental bandgaps that range from 3.1 to 3.6 eV [1, 9], for $BaMoO_4$ from 3.2 to 4.1 eV [11, 12], and for $CdMoO_4$ from 3.3 to 4 eV [13, 14]. This indicates that the bandgap of scheelite-type molybdates cannot be regarded as being accurately determined.

In this letter we shall determine the bandgap of $BaMoO_4$, $CdMoO_4$, and $PbMoO_4$ by employing Urbach's law and we shall also get a deeper insight into the consequences of the presence of Pb $6s$ electrons at the top of the valence band. We shall present optical absorption measurements on scheelite-type $BaMoO_4$, $CdMoO_4$, and $PbMoO_4$ scintillators under compression and pressure dependent electronic band structure, electronic density of states (DOS) and electron localiza-

*Electronic address: Virginia.Monteseguro@uv.es

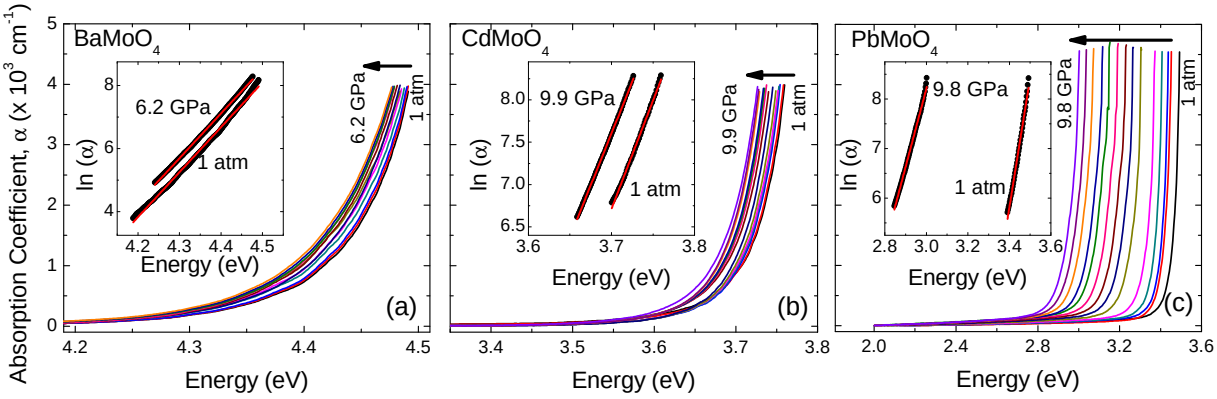

FIG. 1: Optical absorption edges of (a) $BaMoO_4$, (b) $CdMoO_4$, and (c) $PbMoO_4$ from ambient pressure to 6.2, 9.9, and 9.9 GPa, respectively. The arrows indicate the direction in which the spectra move under compression. In the insets, the linear fits of the ln(α) in a semilogarithmic plot of the three compounds at 1 atm and high pressure are represented.

tion function (ELF) calculations.

The optical absorption experiments were performed on $\sim 80 \times 80$ μm^2 crystals platelets with a thickness of $\sim$10 μm^3 obtained from large single crystals grown by the Czochralski method [15]. The optical setup consisted on a confocal system with a deuterium lamp, a fused silica lens, and two Cassegrain objectives for focusing on the sample and collecting the transmitted light. The beam spot size was 50 μm and the spectrometer employed was an UV-VIS OCEAN HR4000. The samples were loaded together with a ruby chip for pressure determination [16] and a mixture of methanol-ethanol-water (16:4:1) as pressure transmitting medium (PTM) in the 250 μm hole of a 40 μm thick stainless-steel gasket placed between the two 500 μm diamonds of a membrane-type diamond anvil cell (DAC).

The electronic band structure and electron charge density calculations at different pressures have been performed within the framework of DFT [17] with the Vienna *ab initio* simulation package (VASP) [18–21]. Projector augmented wave (PAW) [22] pseudopotentials were used and the set of plane waves were extended up to a cutoff of 520 eV. The exchange-correlation energy was described with a generalized gradient approximation (GGA) within the PBEsol prescription [23]. The integrations over the Brillouin zone (BZ) of the scheelite structures were carried out with a dense grid of special k-points (4×4×4) employing the Monkhorst-Pack method [24]. The convergence achieved was 1-2 meV per formula unit in the total energy, the forces on the atoms were almost negligible (smaller than 0.005 eV/$\mathring{A}$) and the deviations of the stress tensor from its diagonal hydrostatic form minimal (lower than 0.1 GPa). In order to analyze the electronic structure, we have resorted to quantum topology. We have used the electron density and its critical points, noticeable the first order critical points, also known as bond critical points (bcps) within the Quantum Theory of Atoms in Molecules.[25] The delocalization and sharing of electrons was evaluated thanks to the Electron Localization Function (ELF) [26, 27]. The ELF enables to highlight the change in kinetic energy density due to the Pauli principle, thus providing a picture in terms of electron pairs. Data were obtained from the numerical analysis of the respective VASP output files (ELFCAR and CHGCAR) with the CRITIC code [28, 29].

The absorption edges of $BaMoO_4$, $CdMoO_4$, and $PbMoO_4$ are shown in Fig. 1 at different pressures in the hydrostatic limit ($\sim$10 GPa) of the PTM used [30]. The steepness of the absorption spectra of the three compounds, with values of the absorption coefficient of $\sim$4500 cm^{-1} for 10 μm thick samples, indicate the direct nature of the transition [8]. A first inspection of the absorption spectra under pressure shows that the absorption edges of the three compounds redshift under compression, but while in the case of $BaMoO_4$ and $CdMoO_4$ the redshift is below 0.05 eV up to $\sim$10 GPa, in the case of $PbMoO_4$ the increase in pressure moves the absorption edge around 0.6 eV to lower energies in the same pressure range.

The absorption edge of scheelites consists of the superposition of a steep absorption from a direct bandgap and a low-energy band related to pre-edge absorptions from defects and impurities [31]. According to previous works [32–34], the steep absorption edge of scheelites exhibits an exponential dependence with energy following Urbach's law [10] as the result of excitonic effects resulting from the dissociation of excitons in the electric fields of polar phonons or impurities. Hence, a typical $(\alpha h\nu)^2$ analysis might lead to either an overestimation or an underestimation of the bandgap depending on the maximum value of the absorption coefficient collected. Should the absorption edge have an exponential dependence with energy, the upper part of the ln(α) would be a straight line with energy. As can be seen in the case of $BaMoO_4$ (Fig. 1), the ln(α) has the same slope at ambient pressure and at 6 GPa, indicating no steepness change under pressure. Therefore, we performed the fits to the absorption edge according to Urbach's law $\alpha = A_0 e^{(-(E_g - h\nu)/E_U)}$, where A_0 is a weight constant usually associated to the quality of the crystals, and E_U is Urbach's energy directly related to the steepness of the spectrum and hence the amount of defects. In Urbach's law there are three parameters to fit; A_0 and E_g are related to the absorption intensity, and E_U is the only parameter from the three ones that can be determined independently from the

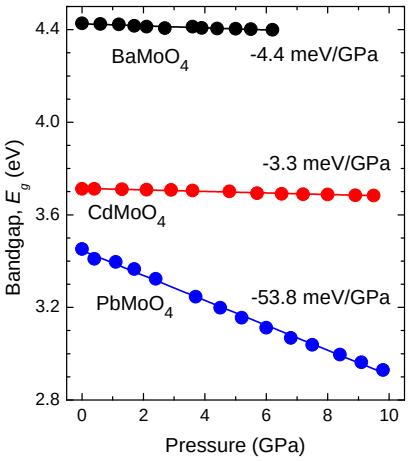

FIG. 2: Pressure dependence of the bandgap E_g of $BaMoO_4$, $CdMoO_4$, and $PbMoO_4$ (filled circles) as obtained from the fits to our spectra.

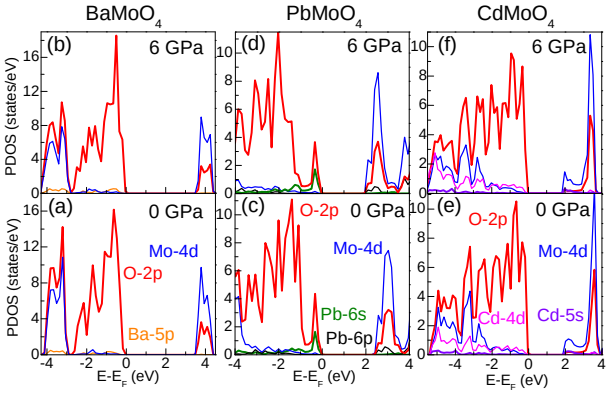

FIG. 3: Electronic partial density of states of $BaMoO_4$ (a) at 0 GPa and (b) at 6 GPa, of $PbMoO_4$ (c) at 0 GPa and (d) at 6 GPa and of $CdMoO_4$ (e) at 0 GPa and (f) at 6 GPa. The $2p$ orbitals of O are represented by red line, the $4d$ orbitals of Mo by blue line, the $5p$ orbitals of Ba by orange line, the $6s$ ($6p$) orbitals of Pb by green (black) line and the $4d$ ($5s$) orbitals of Cd by pink (violet) line.

slope of the semilogarithmic plot (Fig. 1). To perform the fits, we followed the strategy used before in other type of compounds [35, 36], obtaining an estimate value of A_0 = 1200 cm^{-1} for the three compounds which was assumed to be constant with pressure as observed before [7]. We fitted all the spectra, including the one at ambient pressure, fixing A_0 = 1200 cm^{-1} and leaving E_U and E_g free. For E_U we found with pressure almost constant values of 0.06 eV for $BaMoO_4$, and 0.04 eV for $CdMoO_4$ and $PbMoO_4$; in the order of the E_U values previously obtained for scheelite type tungstates [7] and indicative of the steepness of the spectra. Our fits at ambient pressure yield bandgap values for the three compounds of 4.43 eV ($BaMoO_4$), 3.71 eV ($CdMoO_4$), and 3.45 eV ($PbMoO_4$). Larger than those reported before for $BaMoO_4$ [11, 12] and $PbMoO_4$ [9]. The pressure dependence of the bandgaps of the three compounds is shown in Fig. 2. As already observed in Fig. 1, under pressure the bandgap of the three compounds redshifts but while it barely moves with pressure for $BaMoO_4$ (-4.4 meV/GPa) and $CdMoO_4$ (-3.3 meV/GPa), it redshifts at -53.8 meV/GPa for $PbMoO_4$ in good agreement with Jayaraman et al. [9] that found a value of -50 meV/GPa.

The contribution of the atomic orbitals in the band-structure through the partial density of states (pDOS) is shown in Fig. 3. In $BaMoO_4$ and $CdMoO_4$, the valence (VB) and conduction (CB) bands can be mostly understood by considering the $(MoO_4)^{2-}$ ions alone. The top of the VB is dominated by the O^{2-} $2p$ states, while the bottom of the CB consists of the Mo^{6+} $4d$ states [5]. In the case of $PbMoO_4$, the top of VB is also dominated by the $6s$ orbitals of Pb atoms, which overlap with the $O-2p$ states, and the Pb^{2+} $6p$ states are present at the bottom of the CB.

The electronic band-structures of $BaMoO_4$, $CdMoO_4$, and $PbMoO_4$ at ambient pressure and 6 GPa can be seen in Fig. 4. $BaMoO_4$ has a direct bandgap of 3.88 eV located at Γ at ambient pressure, which compares very well with the experimental one mentioned above. According to the calculations its bandgap becomes indirect, from Γ to Z, beyond 4 GPa, although the direct bandgap is the one observed experimentally.In the $CdMoO_4$, the bandgap, of 2.21 eV at 0 GPa, is indirect from Γ to the direction (ΓZ) in the whole range. However, the direct bandgap, the experimentally accessible one, is found at Γ and it is of 2.27 eV at 0 GPa. Finally, the bandgap of $PbMoO_4$ is indirect at the all pressure points, going from the direction Δ to Γ and taking a value of 2.67 eV at 0 GPa. Experimentally, the bandgap observed is the direct one, located at the direction Δ, and it is of 2.71 eV at ambient pressure. In $CdMoO_4$ and $PbMoO_4$, the theoretical bandgap energy is underestimated if we compare it with the experimental values, probably due to the influence of the d orbitals of Cd and Pb atoms at the VB, which do not contribute much to the experimental bandgap. However, the theoretical pressure evolution of the bandgap is in good agreement with our experiments in the three cases. For $BaMoO_4$ and $CdMoO_4$, the bandgaps redshift at -1.1 meV/GPa and -5.8 meV/GPa, respectively. As was noticed experimentally, in the case of $PbMoO_4$, the bandgap decreases abruptly at -70 meV/GPa.

The analysis of the electron density and related scalar fields is shown in Fig. 5. The Laplacian of the electron density at the bcp (electron density saddle point) gives an idea of the ionicity ($\nabla^2\rho > 0$) vs covalency ($\nabla^2\rho < 0$) of a system. When the Laplacian is close to zero, densities are typically very flat (weak bonds or metals). As can be seen in Figure 5 (a), $Cd-O$ interactions are rather ionic ($\nabla^2\rho$ = 0.17 a.u.) whereas the Laplacian at Pb-O and Ba-O interactions ($\nabla^2\rho \approx$ 0.1 a.u.) identifies a rather delocalized interaction. Moreover, looking at the electron density of these two interactions [Fig. 5 (b)], we can see that the interaction in $Ba-O$ is weaker ($\rho =$ 0.026 a.u.) than that of Pb ($\rho = 0.036$ a.u.). Hence, the interactions in the compounds can be relatively classified as ionic for Cd, weak for Ba, and more delocalized for Pb. This interpretation is confirmed by the ELF values at the bcps [Fig. 5 (c)], which are higher for the two stronger compounds (Cd and Pb). In conclusion, in the case of $PbMoO_4$ compound, we describe a delocalized $Pb-O$ bond, due to a high ELF value,

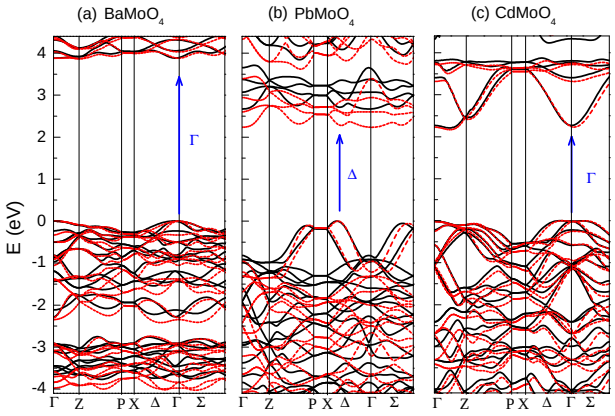

FIG. 4: Electronic band-structure dispersion curves of (a) $BaMoO_4$, (b) $PbMoO_4$ and (c) $CdMoO_4$ at ambient pressure (black) and at 6 GPa (red). The blue arrows indicate where the experimental bandgaps take place

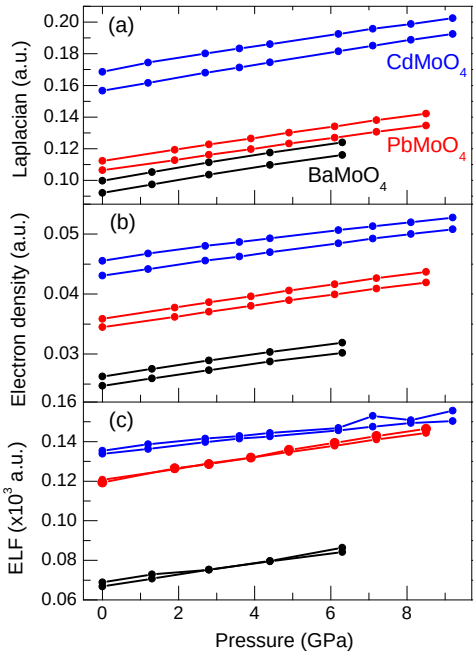

FIG. 5: Pressure evolution at the O$-X$ (X = Cd,Pb,Ba) bond critical points (bcps) of (a) the Laplacian of the electron density, (b) the electron density and (c) the ELF at the bond critical points. The black, red and blue curves correspond to $BaMoO_4$, $PbMoO_4$ and $CdMoO_4$, respectively. The two lines per compound are due the presence of two non-equivalent O$-X$ bcps in the unit cell.

a high electron density and a Laplacian close to zero.

The delocalized densities are associated with the top of the bands, in agreement with the DOS analysis. Moreover, they are more compressible and more reactive (bigger $\partial E/\partial V$), what explain the steeper evolution of the top of the band with pressure. Our DOS and ELF analysis open a new interpretation of the origin of the bandgap of $PbMoO_4$: the charge transfer band in $PbMoO_4$ is most probably taking place between the Pb $6s$ and O $2p$ levels instead of between the O $2p$ and the Mo $4d$ levels as in the rest of free lead molybdates. Such an explanation is also based in the fact that the band gap of these compounds is associated with the behaviour of the local structure of the scheelites under compression. In the scheelite-type molybdate structure, $AMoO_4$, the compressibility is ruled by the dodecahedral AO_8 units since the tetrahedral MoO_4 units are almost incompressible [37, 38]. Therefore, the fast decrease of the bandgap in the $PbMoO_4$ with respect to the other scheelites can be understood considering the energy transition to be from Pb$-6s$ to O$-2p$ bands within the PbO_8 dodecahedra, which is more sensitive to the increase of the pressure than the O$-2p$ to Mo$-4d$ transition, constrained to the MoO_4 tetrahedra, as in $BaMoO_4$ and $CdMoO_4$. Furthermore, taking into account that the crystal structure of scheelites (space group $I4_1/a$) is centrosymmetric and the $s-p$ mixing is forbidden at zone center, this would explain why the direct bandgap of $PbMoO_4$ takes place at Δ instead of at zone center as in $BaMoO_4$ and $CdMoO_4$.

In conclusion, we have accurately determined the bandgaps and pressure derivatives of $BaMoO_4$, $PbMoO_4$, and $CdMoO_4$ crystals by means of the linear fit of their absorption edges to Urbach's law finding that the bandgap of $PbMoO_4$ reacts one order of magnitude faster than in the lead-free molybdates. Such a feature is well explained if we consider that the transition occurs between Pb-$6s$ levels in VB and O-$2p$ levels in CB. Such a transition is more sensitive to compression changes due to its high electron delocalization and the high compressibility of dodecahedral PbO_8 units in the scheelite-type tetragonal structure. This charge transfer band is confirmed by the *ab initio* DOS and ELF calculations and it is allowed since it fulfills the electric dipole selection rules. This transition explains that the bandgap occurs in the direction Δ instead of the zone center as expected in a centrosymmetric structure in which $s-p$ mixing is not allowed at zone center. Finally, our results can be directly extended to $BaWO_4$, $PbWO_4$ and $CdWO_4$ which show an identical electronic band structure.

V.M. acknowledges the Spanish MCIU for the Juan de la Cierva Program (FJCI-2016-27921). This project was funded by the Spanish MCIU, the Spanish Research Agency (AEI), and the European Fund for Regional Development (FEDER) through the project MAT2016-75586-C4-1/3-P, and by the Generalitat Valenciana through the grant Prometeo/2018/123 EFIMAT.

[1] M. Fujita, M. Itoh, H. Mitani, Sangeeta, and M. Tyagi, Phys. Stat. Sol. B **247**, 405 (2010).
[2] M. Kirm, V. Nagirnyi, E. Feldbach, M. D. Grazia, B. Carré, H. Merdji, S. Guizard, G. Geoffroy, J. Gaudin, N. Fedorov, et al., Phys. Rev. B **79**, 233103 (2009).
[3] S. Rathee, D. Tu, T. T. Monajemi, D. W. Rickey, and B. G.

Fallone, Med. Phys. **33**, 1078 (2006).
[4] M. M. Silva, S. M. V. Novais, E. S. S. Silva, T. Schimitberger, Z. S. Macedo, and R. F. Bianchi, Mater. Chem. Phys. **136**, 317 (2012).
[5] Y. Zhang, N. A. W. Holzwarth, and R. T. Williams, Phys. Rev. B **57**, 12738 (1998).
[6] Y. Abraham, N. A. W. Holzwarth, and R. T. Williams, Phys. Rev. B **62**, 1733 (2000).
[7] R. Lacomba-Perales, D. Errandonea, A. Segura, J. Ruiz-Fuertes, P. Rodríguez-Hernández, S. Radescu, J. López-Solano, A. Mújica, and A. Muñoz, J. Appl. Phys. **110**, 043703 (2011).
[8] D. Errandonea, D. Martínez-García, L. Lacomba-Perales, J. Ruiz-Fuertes, and A. Segura, Appl. Phys. Lett. **89**, 091913 (2006).
[9] A. Jayaraman, B. Batlogg, and L. G. V. Uiert, Phys. Rev. B **31**, 5423 (1985).
[10] F. Urbach, Phys. Rev. **92**, 1324 (1953).
[11] J. K. Thomas, S. Vidya, S. Salomon, and K. Joy, Conf. Series: Materials Science and Engineering **23**, 012031 (2011).
[12] J. C. Sczancoski, L. S. Cavalcante, N. L. Marana, R. O. da Silva, R. L. Tranquilin, M. R. Joya, P. S. Pizani, J. A. Varela, J. R. Sambrano, M. Siu, et al., Curret Appl. Phys **10**, 614 (2010).
[13] W. Ran, H. M. Noh, S. H. Park, B. K. Moon, J. H. Jeong, J. H. Kim, and J. Shi, Sci. Reports **8**, 5936 (2018).
[14] M. Fujita, M. Itoh, T. Katagiri, D. Iri, M. Kitaura, and V. Mihkailik, Phys. Rev. B **77**, 155118 (2008).
[15] V. B. Mikhailik, H. Kraus, D. Wahl, and M. S. Mykhaylyk, Phys. Stat. Sol. B **242**, R17 (2005).
[16] H. K. Mao, J. Xu, and P. M. Bell, J. Geophys. Res. **91**, 4673 (1986).
[17] P. Hohenberg, Phys. Rev. **136**, 864 (1964).
[18] G. Kresse and J. Hafner, Phys. Rev. B **49**, 14251 (1994).
[19] G. Kresse and J. Hafner, Phys. Rev. B **49**, 14251 (1994).
[20] G. Kresse and J. Furthmüller, J. Comput. Mat. Sci. **6**, 15 (1996).
[21] G. Kresse and J. Furthmüller, Phys. Rev. B **54**, 11169 (1996).
[22] P. E. Blöchl, Phys. Rev. B **50**, 17953 (1994).
[23] J. P. Perdew, A. Ruzsinszky, G. I. Csonka, O. A. Vydrow, G. E. Scuseria, L. A. Constantin, X. Zhou, and K. Burke, Phys. Rev. Lett. **100**, 136406 (2008).
[24] H. J. Monkhorst and J. D. Pack, Phys. Rev. B **13**, 5188 (1976).
[25] R. F. W. Bader (1990).
[26] A. D. Becke and K. E. Edgecombe, J. Chem. Phys. **92**, 5397 (1990).
[27] B. Silvi and A. Silvi, Nature **371**, 683 (1994).
[28] A. O. de-la Roza, J. Contreras-Garcia, and E. R. Johnson, Phys. Chem. Chem. Phys. **185**, 1007 (2014).
[29] A. O. de-la Roza, E. R. Johnson, and V. Luaña, Comput. Phys. Commun. **185**, 1007 (2014).
[30] R. J. Angel, M. Bujak, J. Zhao, G. D. Gatta, and S. D. Jacobsen, J. Appl. Cryst. **40**, 26 (2007).
[31] M. Nikl, Phys. Stat. Sol. A **178**, 595 (2000).
[32] M. Itoh, T. Katagiri, Y. Tani, and M. Fujita, Radiat. Meas. **42**, 545 (2007).
[33] M. H. M. F. M. Itoh, H. Yokota and Y. Usuki, Phys. Stat. Sol. B **231**, 95 (2002).
[34] M. Fujita, M. Itoh, M. Horimoto, and H. Yokota, Phys. Rev. B **65**, 195105 (2002).
[35] J. Ruiz-Fuertes, A. Friedrich, D. Errandonea, A. Segura, W. Morgenroth, P. Rodríguez-Hernández, A. Muñoz, and Y. Meng, Phys. Rev. B **95**, 174105 (2017).
[36] J. Ruiz-Fuertes, O. Gomis, A. Segura, M. Bettinelli, M. Burianek, and M. Mühlberg, Appl. Phys. Lett. **112**, 042901 (2018).
[37] L. F. R. M. Hazen and J. W. E. Mariathasen, J. Chem. Phys. Solids **46**, 253 (1985).
[38] D. Errandonea, J. Pellicer-Porres, F. J. Manjón, A. Segura, C. Ferrer-Roca, R. S. Kumar, O. Tschauner, J. López-Solano, P. Rodríguez-Hernández, S. Radescu, et al., Phys. Rev. B **72**, 174106 (2005).